Preprints of the 21st IFAC World Congress (Virtual)
Berlin, Germany, July 12-17, 2020

Variable-Impedance and Force Control for Robust Learning of Contact-rich Manipulation Tasks from User Demonstration

Nima Enayati*, Stefano Mariani, Arne Wahrburg*, Andrea M. Zanchettin****

**ABB Corporate Research, Ladenburg, Germany*
{nima.enayati, arne.wahrburg} @de.abb.com
*** Politecnico di Milano, Milan 20133, Italy*
stefano17.mariani@mail.polimi.it, andreamaria.zanchettin@polimi.it

Abstract: This paper proposes a Cartesian variable-impedance and force controller that enables manipulators to track position and force references demonstrated by a user through kinesthetic teaching. The proposed approach deploys the variability of user demonstrations to adapt the compliance profile of the manipulator to uncertainties and utilizes interaction force measurements during task reproduction to enhance force tracking performance. A passivity analysis is provided to demonstrate the stability of the system and a simulation exemplifies how passivity is achieved in the presence of variable impedance and force feedback. Furthermore, using a 7-DOF manipulator equipped with a force sensor, two experiments were conducted to highlight the ability of the proposed approach in successfully reproducing tasks with disturbances, where the state-of-the-art methods fall short.

Keywords: Teaching by demonstration, Impedance control, Co-Learning and self-learning; Motion Control Systems; Intelligent robotics

1. INTRODUCTION AND STATE OF THE ART

Today, most robots deployed in industrial applications such as assembly are position-controlled and programmed to follow user-defined trajectories. Theses robots offer precise and high-bandwidth position and velocity control that can increase productivity and accuracy. Such automation solution require cumbersome robot programming and utmost care in assembly-line design to minimize variation in the involved parts and the environment, as minute deviations from assumed geometries and constraints may lead to a failure of the program and thus bringing production to a halt. Reducing the required effort in setting up an automated robotic task and at the same time achieving a high degree of robustness to uncertainties has been a topic of interest to the industries and academia for decades. Programming by Demonstration (PbD) (Billard et al. 2008) methods aim at simplifying the traditional means of programming a robot, by capturing user demonstrations of a task using a variety of sensing schemes and encode these demonstrations through a mathematical representation that can be used by the robot to reproduce the task. Kinesthetic teaching, where the user moves a gravity-compensated robot by hand to demonstrate the desired motion is one of the more common input methods in PbD (Argall et al. 2009). Several solutions for encoding demonstrated trajectories have been proposed including Dynamic Movement Primitives (DMP) (Schaal 2006), Probabilistic Movement Primitives (Paraschos et al. 2013), and Gaussian Mixture Model (GMM) (Calinon et al. 2010) (Khansari-Zadeh and Billard 2011), where the latter provides an intuitive representation of the variance among multiple demonstrations of users. Such stochastic information can be exploited to increase the robustness of the system, as will be discussed shortly. Although generating and tracking pose trajectories from user demonstrations can speed-up the traditional point-to-point robot programming, intricate robotic tasks that encompass contact with the environment will still require elaborate programming and possibly switching to force control for segments of the task. One might resort to impedance control (Hogan 1985) which is one of the more popular approaches that can implicitly regulate interactions with the environment and enhance robustness. In impedance control, the objective of purely controlling pose is replaced with that of controlling the impedance of the robot-environment interaction through imposing a mass-spring-damper disturbance response. Inspired by the ability of biological motor control in adapting the impedance of the overall biomechanical system to different task requirements and disturbances, several works have proposed impedance controllers with varying stiffness (Buchli et al. 2011), (Kronander and Billard 2012). Variable impedance can enhance the robustness of the system with respect to geometrical uncertainties. In addition, increasing the compliance when accurate positioning is not needed can prevent the robot from applying excessive force to the environment. This can diminish the severity of accidental collisions with users, prevent unnecessary safety breaks engagement when in unexpected contact with the environment, and reduce the probability of damaging the workpieces or the robot.

When the demonstrated task includes parts where close tracking of interaction force is of importance, an impedance controller proves to be of limited use. Knowing the environment's geometry and mechanical properties, one can set the stiffness and the position references (on a flat surface, for example, references would be set below the actual surface) to generate a specific interaction force (Zeng and Hemami 1997). Such extensive knowledge of the environment reduces practical applicability of this implicit force controller. To

counter this issue Calinon *et al.* (Kormushev, Calinon, and Caldwell 2011) introduced a variable stiffness controller which is augmented with a feed forward force reference. During user demonstrations, only the position information is recorded, and the force information is acquired when the robot reproduces the demonstration for the first time while the user remotely uses a haptic device to enter desired forces. While such an acquisition protocol might suffice for simple tasks such as the ironing task reported in (Kormushev et al. 2011), an end-effector mounted Force/Torque (F/T) sensor allows to remain within the more intuitive kinesthetic teaching framework and simultaneously acquire pose and force measurements of intricate tasks in one shot (user handles the manipulator at any point before the mounted F/T sensor). In (Montebelli, Steinmetz, and Kyrki 2015) such an acquisition platform was used to record user demonstrations and DMP was deployed to generate desired pose and force trajectories (only in a single Cartesian dimension). Based on whether the magnitude of the force reference is equal to zero or not, the proposed controller switched between an impedance controller with pose references and a pure 1-dimensional force feedforward. The work was extended in (Racca et al. 2016) to include 3D Cartesian force and to replace the simple controller switching method with a hidden semi-Markov model to classify 2 states of *contact* or *no-contact* and smoothly transition between impedance control and force feed-forward by modifying the stiffness matrix of the impedance controller. These approaches are based on the implicit assumption that interaction forces are only of interest when non-zero values are recorded during the demonstration. However, the absence of external forces during the demonstration is itself an information that can be exploited if non-zero external forces are encountered during the task replication by the robot. In fact, to the best of our knowledge, none of the works in the PbD literature that regard force and position learning, utilize interaction force measurement during the entirety of task replication. In the absence of force feedback, the accuracy of the force tracking can be largely limited as the controller must rely on open loop feedforward force reference. As we will demonstrate in this paper, a more accurate force tracking not only matters for explicit force control tasks, but it can enable the robot to successfully reproduce tasks where force references are zero, and at which current PbD methods can fall short. The presence of force feedback loop in addition to position feedback in the impedance controller can affect the stability of the system and stability analysis cannot be neglected (Schindlbeck and Haddadin 2015). In fact system stability can also be jeopardized when arbitrary variations of the impedance parameters are allowed (Kronander and Billard 2016) (Ferraguti, Secchi, and Fantuzzi 2013). However, the risk of encountering instability has rarely been explicitly addressed in the PbD works that deploy variable impedance controllers.

In this work, we introduce a PbD framework that utilizes GMM/GMR to encode Cartesian positions and interaction forces of user demonstrations and to generate desired references for position, force, and Cartesian stiffness. These desired references are then regulated by a controller which is augmented by a passivity observer to guarantee stability. The main contribution of this work is a variable Cartesian impedance and force controller that aims at increasing the tracking accuracy of interaction force in PbD. Furthermore, stability analyses and a passivity observer is provided for the impedance and force controller in presence of force feedback and variable stiffness. The paper is structured as follows. Section 2 contains a preliminary introduction to the models used in this work and detailed discussion of the proposed method. In Section 3, simulation and experimental results are provided and discussed. Section 4 provides conclusions and directions for future works.

2. METHODS

2.1 Robot dynamic model

We consider the dynamic model of an n-DOF (Degree of Freedom) manipulator (Siciliano et al. 2009) with rigid joints described as:

$$M(q)\ddot{q} + C(q,\dot{q})\dot{q} + g(q) = \tau_c + \tau_{ext} \quad (1)$$

Where $q \in R^n$ is the vector of joint variables, $M(q) \in R^{nxn}$ is the positive definite inertia matrix, $C(q,\dot{q})\dot{q} \in R^n$ is the Coriolis and centrifugal torques vector, $g(q) \in R^n$ is the gravitational torque, $\tau_c \in R^n$ the torque commanded by the controller, and $\tau_{ext} \in R^n$ is the torque from interaction with the environment. The scope of this paper is limited to position and interaction force. However, the proposed formulation can be extended to include full pose and interaction wrench. The corresponding dynamic model in task space (Khatib 1995) considering only translation is given as:

$$\Lambda(x)\ddot{x} + \mu(x,\dot{x})\dot{x} + F_g(x) = F_c + F_{ext} \quad (2)$$

where $x \in R^3$ is the cartesian position vector of the end effector obtained through forward kinematics from the joint vector q, $\Lambda = (JM^{-1}J^T)^{-1} \in R^{3x3}$ is the end effector inertia matrix with $J(q) \in R^{3\times n}$ being the Jacobian matrix of the manipulator at joint configuration q, $\mu(x,\dot{x})\dot{x} = \Lambda(JM^{-1}C - \dot{J})\dot{q}$, $F_g = J^{-T}g$, $F_c = J^{-T}\tau_c$ and $F_{ext} = J^{-T}\tau_{ext}$ all $\in R^3$.

2.2 Trajectory encoding and reference generation

In programming by demonstration, the trajectories acquired from user demonstrations are first encoded through a mathematical representation that can extract the fundamental features of the desired task. In this work, we utilize GMMs to encode demonstrations and Gaussian Mixture Regression (GMR) to generate reference trajectories from the derived GMMs. Further details of these methods can be found in the literature (Calinon, Guenter, and Billard 2007). In addition to position trajectories, we encode the interaction force profile of the tool with the environment recorded during the demonstration, using an end-effector mounted force sensor. Furthermore, we utilize the covariance of the provided position trajectories, to define a time varying stiffness and damping profile for the impedance controller, as will be described in Subsection 2.3.

Acquired demonstrations are commonly aligned in time using methods such as dynamic time warping or cross-correlation analysis (Calinon 2016). The optimal number of Gaussians to fit the demonstrated data is found through Bayesian Information Criterion (BIC) (Calinon et al. 2007) to have a

tradeoff between model error and model complexity. Given a position and a force datasets of N points that share the time vector t_j: $\xi_j = \{t_j, x_j\}_{j=1}^{N}$,$\varphi_j = \{t_j, f_j\}_{j=1}^{N}$, two mixtures of M_x gaussians described by $\{\pi_{x,i}, \mu_{x,i}, \Sigma_{x,i}\}_{i=1}^{M_x}$ for position and M_f gaussians described by $\{\pi_{f,i}, \mu_{f,i}, \Sigma_{f,i}\}_{i=1}^{M_f}$ for force are generated, where π_i represents the priors, μ_i is mean and Σ_i the covariance matrix of the i^{th} gaussian. Training of the mixtures is done with the Expectation Maximization (EM) algorithm, initialized with the K-mean clustering techniques to avoid getting trapped in local minima (Bishop 2006). Applying GMR on these two mixtures of gaussians, and using the temporal components as query points, we obtain the profiles of the desired position $x_d(t)$, desired force $F_d(t)$ and the corresponding covariance matrices $\Sigma_x(t)$ and $\Sigma_f(t)$ that are then used to control the robot.

2.3 Controller definition

In the classic impedance controller (Hogan 1985):

$$F_c = -K_x\tilde{x} - D_x\dot{\tilde{x}} + \Lambda(x)\ddot{x}_d + \mu(x,\dot{x})\dot{x}_d + F_g(x) \quad (3)$$

where $\tilde{x}(t) = x(t) - x_d(t)$ is deviation from desired position, and K_x and D_x are stiffness and damping values (often diagonal), the interaction force with the environment is an indirect result of the position error and the stiffness gains. To provide the option of including desired force references, in (Kormushev et al. 2011), (Montebelli et al. 2015), and (Racca et al. 2016) a desired force term F_d was added to the controller:

$$F_c = -K_x\tilde{x} - D_x\dot{\tilde{x}} + F_d + \Lambda(x)\ddot{x}_d + \mu(x,\dot{x})\dot{x}_d + F_g(x) \quad (4)$$

However, since such a controller relies on a feedforward force reference, disturbances in the environment can hinder the ability of the controller in delivering a robust force tracking performance. Towards achieving a variable impedance and force controller for PbD applications with improved robustness to uncertainties, we propose the following variable gain controller:

$$F_c = -K_x\tilde{x} - D_x\dot{\tilde{x}} + F_d + K_f(F_{ext} - F_d) + \Lambda(x)\ddot{x}_d + \mu(x,\dot{x})\dot{x}_d + F_g(x) \quad (5)$$

where the proportional feedback term $K_f(F_{ext} - F_d)$ can enhance the reference force tracking performance. Unlike the controller proposed in (Schindlbeck and Haddadin 2015), here the controller gains are variable and adapted to emphasis force or position regulation, as will be shortly discussed. The proposed controller leads to the following relation between the pose error and the external force:

$$\Lambda(x)\ddot{\tilde{x}} + \big(D_x + \mu(x,\dot{x})\big)\dot{\tilde{x}} + K_x\tilde{x} = F_{ext} + F_d + K_f(F_{ext} - F_d) \quad (6)$$

maintaining and balancing the desired spring-damper dynamic relation between external force and the position/velocity error and reference forces, while a full-body compliance is guaranteed. To obtain an ideal impedance behaviour, also the inertial terms in equation (1) can be compensated through inertia reshaping. However, for lightweight manipulators in collaborative applications, this term is practically negligible due to relatively low inertias and accelerations. In (6), the stiffness K_x can act as a weighting term between position and force error, allowing to prioritize the tracking of either. In the following we describe our approach to generate a smooth stiffness profile that is deduced from the demonstrated position and force trajectories.

As previously discussed in literature, variance of the demonstrated trajectories can be interpreted as the importance of accurate tracking for the user. In other words, if a section of the motion is consistent among different demonstrations then it can be deduced that the section is likely to benefit from higher position tracking performance, while in the presence of high variability in the demonstrations, position tracking can be relaxed and other constraints of the task can be emphasized. This can be achieved by defining the stiffness proportionally to the inverse of the observed covariance $(\Sigma_{x,i})^{-1}$:

$$K(t) = \sum_{i=1}^{K} h_i(t)\, K_i \quad (7)$$

where K_i and $h_i(t)$ are respectively the stiffness associated to each gaussian i of the GMM and a weighting term defined as:

$$K_i = V_i B_i V_i^{-1} \qquad h_i(t) = \frac{\mathcal{N}\big(\boldsymbol{x_t}\big|\boldsymbol{\mu}_i, \boldsymbol{\Sigma}_i\big)}{\sum_{i=1}^{K}\mathcal{N}\big(\boldsymbol{x_t}\big|\boldsymbol{\mu}_i, \boldsymbol{\Sigma}_i\big)} \quad (8)$$

$$B_i = K_{min} + (K_{max} - K_{min})\frac{\lambda_i - \lambda_{min}}{\lambda_{max} - \lambda_{min}} \quad (9)$$

where V_i and λ_i are the eigenvectors and eigenvalues obtained through the eigen components decomposition of the inverse of the covariance matrix associated to each Gaussian $(\Sigma_{x,i})^{-1}$. Equation (9) normalizes each eigenvalue the minimum and maximum eigenvalues observed among the Gaussians in all the three Cartesian directions, and maps them to the range of minimum and maximum stiffness $[K_{min}\ \ K_{max}]$ selected by the user. If K_{min} is set to zero, the controller may stop tracking position references in the presence of high demonstration variance. Note that stiffness is defined independently for all Cartesian dimensions.

We furthermore modify the stiffness profile to reflect the priority of force tracking, simply based on the magnitude of the force F_t after it is normalized:

$$K_x(t) = K(t) * \left(\gamma_{max} + (\gamma_{min} - \gamma_{max})\left(\frac{F_{max} - |F_{t_i}|}{F_{max} - F_{min}}\right)\right) \quad (10)$$

The values of F_{min} and F_{max} are chosen based on the manipulator and the expected maximum interaction forces. The scaling factors γ_{max} and γ_{min} are respectively the maximum and minimum reduction of the stiffness in correspondence of the maximum and minimum force. This linear reduction of the stiffness removes the necessity of classifying contact and switching controllers as suggested in (Racca et al. 2016). Finally, having the stiffness profile $k_x(t)$, $D_x(t)$ is calculated to obtain a critically damped system (Ott 2008).

2.4 Stability Analysis

In order to analyse the stability of the presented system while interacting with the environment, we exploit the concept of passivity (Shahriari et al. 2017). A system with the state space model $\dot{x} = f(x,u)$ and output equation $y = h(x,u)$, where x

is the state vector subjected to initial condition $x(t_0) = x_0$ and u the input vector, is said to be passive if there exist a positive semidefinite function $S(x)$, called storage function, such that:

$$S\big(x(t_i)\big) - S(x_0) \leq \int_0^{t_i} u^T(t)\, y(t)\, dt \tag{11}$$

for all input signals $u \in [0, t_i]$ and initial states x_0 with $t_i > 0$. Thus proving the passivity is equivalent to finding a storage function $S(x)$ such that:

$$\dot{S} \leq u^T y \quad \forall\, u, y \tag{12}$$

An important property of passivity is that it is additive, so the interconnection of passive systems leads to an overall passive system. The environment is assumed passive with respect to the pair $[\dot{x}, -F_{ext}]$. Hence, we must show the passivity of the modified force-impedance controller. Standard Impedance control with constant stiffness and damping is passive. (Kronander and Billard 2016). However, the passivity cannot be guaranteed in the case of varying impedance and our added force feedback term. As has been shown in the literature for similar controllers (Shahriari et al. 2017), the controller can be augmented with a passivity observer to guarantee stability. Consider the storage function:

$$V(x, \dot{x}) = \frac{1}{2}\dot{\tilde{x}}^T \Lambda(x) \dot{\tilde{x}} + \frac{1}{2}\tilde{x}^T K_x \tilde{x} \tag{13}$$

and its time derivative:

$$\dot{V} = \dot{\tilde{x}}^T \Lambda(x) \ddot{\tilde{x}} + \frac{1}{2}\dot{\tilde{x}}^T \dot{\Lambda}(x) \dot{\tilde{x}} + \tilde{x}^T K_x \dot{\tilde{x}} + \frac{1}{2}\tilde{x}^T \dot{K}_x \tilde{x} \tag{14}$$

Substituting $\ddot{\tilde{x}}$ from (6), considering the skew symmetry property of $\dot{\Lambda}(x) - 2\mu(x, \dot{x})$ and the symmetry of K_x we obtain:

$$\begin{aligned} \dot{V} = {} & \dot{\tilde{x}}^T F_{ext} - \dot{\tilde{x}}^T D_x \dot{\tilde{x}} + \dot{\tilde{x}}^T F_d + \\ & \dot{\tilde{x}}^T K_f (F_{ext} - F_d) + \frac{1}{2}\tilde{x}^T \dot{K}_x \tilde{x} \end{aligned} \tag{15}$$

In case of standard impedance control with constant stiffness, last three terms disappear, and the system is always passive with respect to $[\dot{\tilde{x}}, F_{ext}]$ since:

$$\dot{V} = \dot{\tilde{x}}^T F_{ext} - \dot{\tilde{x}}^T D_x \dot{\tilde{x}} \leq \dot{\tilde{x}}^T F_{ext} \tag{16}$$

However, by adding the force reference terms and variable stiffness, (12) cannot be always guaranteed. Using the concept of an *energy tank* (Ferraguti et al. 2013) (Shahriari et al. 2017) (Schindlbeck and Haddadin 2015), we can virtually store the energy dissipated by the term $\dot{\tilde{x}}^T D_x \dot{\tilde{x}}$ and use it to account for the energy injection of the non-passive terms, therefore the system will remain passive as long as the dissipated energy is able to compensate for the extra injected one. Towards this, we define a tank, whose energy level is $T = 1/2\, x_t^2$ with x_t representing the tank state. The augmented model becomes:

$$\begin{aligned} & \Lambda(x)\ddot{\tilde{x}} + \big(D_x + \mu(x, \dot{x})\big)\dot{\tilde{x}} + K_0 \tilde{x} + \alpha K' \tilde{x} = \\ & F_{ext} + \gamma F_d + \alpha(1-\gamma)F_d + \alpha K_f (F_{ext} - F_d) \\ & \dot{x}_t = \frac{\beta}{x_t}\big(\dot{\tilde{x}}^T D_x \dot{\tilde{x}} - \gamma \dot{\tilde{x}}^T F_d\big) - \\ & \frac{\alpha}{x_t}\big(\dot{\tilde{x}}^T K_f (F_{ext} - F_d) + (1-\gamma)\dot{\tilde{x}}^T F_d - \tilde{x}^T K' \dot{\tilde{x}}\big) \end{aligned} \tag{17}$$

where $K_x(t) = K_0 + K'(t)$ with K_0 representing the constant part of the variable stiffness. The factor β prevents excessive tank storage, by saturating the storage at T_{max}:

$$\beta = \begin{cases} 1 & if\ T \leq T_{max} \\ 0 & else \end{cases} \tag{18}$$

The factor α prevents further injection of energy into the system by the non-passive terms when the dissipated energy accumulated up to that moment has been consumed (that is a minimum admissible level in the tank is reached). This is done by detaching the force controller and the variable stiffness terms:

$$\alpha = \begin{cases} 1 & if\ T \geq T_{min} \\ 0 & else \end{cases} \tag{19}$$

with $T_{min} > 0$ to avoid singularities. The factor γ allows the controller to keep deploying the feedforward force reference term even in the case of a drained tank, if the term is dissipative:

$$\gamma = \begin{cases} 1 & if\ \dot{\tilde{x}}^T F_d < 0 \\ 0 & else \end{cases} \tag{20}$$

The augmented system is now passive with respect to $[\dot{\tilde{x}}, F_{ext}]$. Considering the storage function:

$$S = \frac{1}{2}\dot{\tilde{x}}^T \Lambda(x) \dot{\tilde{x}} + \frac{1}{2}\tilde{x}^T K_0 \tilde{x} + T \tag{21}$$

we can obtain:

$$\begin{aligned} \dot{S} = {} & \dot{\tilde{x}}^T F_{ext} - \dot{\tilde{x}}^T D_x \dot{\tilde{x}} + \gamma \dot{\tilde{x}}^T F_d + \beta(\\ & \dot{\tilde{x}}^T D_x \dot{\tilde{x}} - \gamma \dot{\tilde{x}}^T F_d) \end{aligned} \tag{22}$$

Since $\beta \in [0\ 1]$ we have $\dot{S} \leq \dot{\tilde{x}}^T F_{ext}$ and passivity is guaranteed. The complete control law becomes:

$$\begin{aligned} F_c = {} & -K_0 \tilde{x} - \alpha K' \tilde{x} - D_x \dot{\tilde{x}} + \gamma F_d + \alpha(1-\gamma)F_d \\ & + \alpha K_f (F_{ext} - F_d) + \Lambda(x)\ddot{x}_d + \mu(x, \dot{x})\dot{x}_d + F_g(x) \end{aligned} \tag{23}$$

Through this augmented system we can perform the stiffness variation and the force control passively: when the tank is fully drained, that is we are close to lose the passivity, the force control is deactivated (with the exception of the feedforward term that depend also on γ) and a constant stiffness K_0 is implemented up to the moment that some energy is available in the tank.

3. RESULTS

We present the results of a 1-DOF simulation to show the stability of the proposed controller, followed by experimental validation on two Cartesian tasks using a 7DOF manipulator equipped with a force sensor at its end-effector.

3.1 Simulation results

To validate the effectiveness of the passivity observer, we conducted a simulation deploying the proposed controller on a single joint of an industrial manipulator modelled as a 2-mass, spring and damper system, using the parameters of the first joint of the 2-DOF model described in (Moberg, Öhr, and Gunnarsson 2008). Joint angle and stiffness references were set as the following sinusoids:

$$x_d(t) = 2\sin(0.2t) \quad [rad] \tag{24}$$

$$K_x(t) = 2000 + 700sin(4t) \quad [N.m/rad] \tag{25}$$

Damping was set as $0.2\,N.m.s/rad$, $K_0 = 600\,N.m/rad$ and a constant external force of $80\,N$ was assumed to be applied on the link. The results shown in Figure 1 demonstrate the effects of the passivity observer engagement, limiting the stiffness variation when the system risks losing passivity. As shown on the left plots, the unsupervised variable stiffness results in an unstable interaction. The oscillations in joint angle tracking in the case with passivity observer shown on the right are expected and are due to the high magnitude sinusoidal variation of the stiffness and the elasticity of the simulated joint.

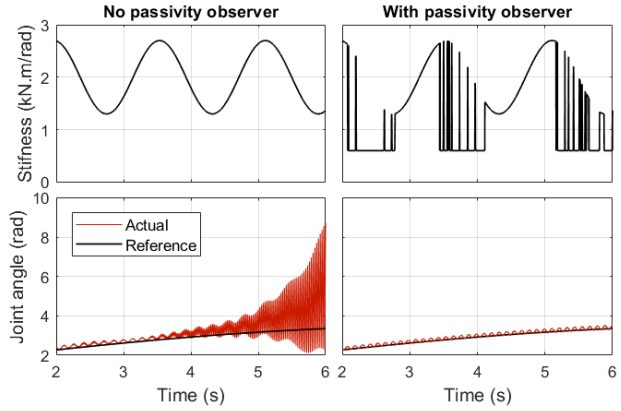

Figure 1 Simulation results of the modelled single joint under the proposed controller with and without passivity observer.

3.2 Experimental results

An experimental setup was prepared to put the proposed controller to test. A 7-DOF research prototype manipulator equipped with a force/torque sensor (Nano 17, ATI Industrial Automation) was controlled via Ethernet at 1 kHz. In terms of controller parameters, we set F_{min} and F_{max} as 0N and 100N, γ_{max} and γ_{min} were 0.4 and 1.0, $K_{min} = 400\frac{N}{m} and \;\; K_{max} = 3000N/m,$ and $K_f = 0.5$. Two tasks were considered. In the first task, the user guided the manipulator from various starting positions over a button (Figure 2), pressed down on the button to engage it, and then guided the manipulator to various final positions. In the second task, the user guided the robot from different starting positions and approached the upper surface of a plastic box. Then the user pressed the tool on the surface while moving along an imaginary line (the orange line shown in Figure 2) on the surface. Finally, the manipulator was guided to the entrance of a hole (1.5mm clearance in radius) and the peg was inserted in the hole. Note that the user hand-guided the robot without touching the force sensor or the tool, so that the sensor only measured the interaction forces with the environment. The pressing section was included in the peg-in-hole experiment, to evaluate the force tracking performance of each controller. Six demonstrations of each task were recorded, the position trajectories of which are shown in Figure 3. The orientation of the end-effector was kept constant. The recorded position trajectories and force profiles of each task were aligned in time with cross-correlation analysis and were then encoded through GMM. To reproduce the encoded tasks, a 9D trajectory was generated encompassing 3D vectors of position, force and cartesian stiffness. The GMR-generated position trajectories are shown as solid red lines in Figure 3. To depict the effects of the proposed method of reducing Cartesian stiffness according to demonstrated interaction forces (Eq. (10), Figure 4 shows the unmodified stiffness trajectories generated based on position variance (dashed black lines) and those augmented with the interaction-force-reduction method (solid red lines) for the peg-in-hole task.

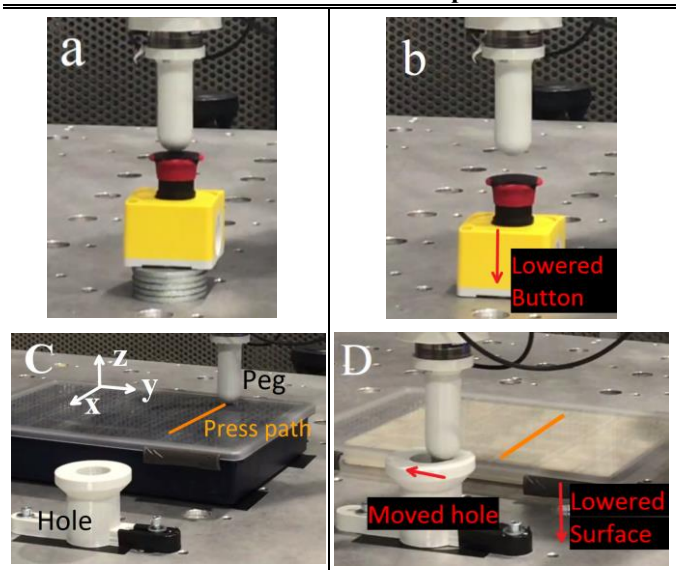

Figure 2 The experimental setup in both disturbed and undisturbed cases.

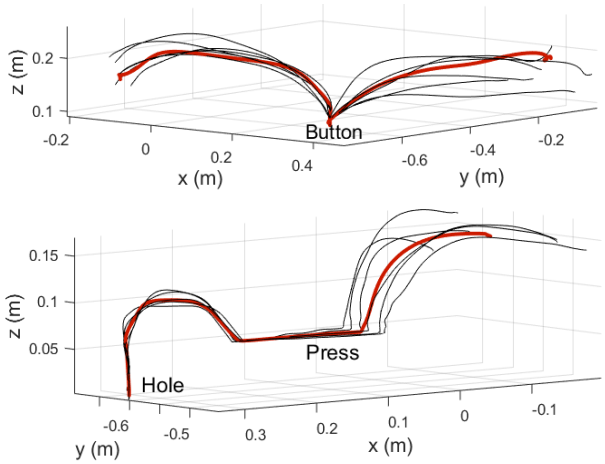

Figure 3 The demonstrated position trajectories (in black) for the button task (above) and the peg-in-hole (below). Red line represents the GMR-generated trajectory from the recorded demonstrations.

Considering the unmodified stiffness trajectories, as expected the stiffness along z dimension is increased in the pressing section since the peg is pressed and moved along the surface and resulting in little variation along the z direction among the demonstrated position trajectories. Similarly, in the peg insertion the stiffness is increased along x and y, as all demonstrations converge to the xy position of the hole. However, thanks to the interaction-force-reduction, the

stiffness values along z are reduced in the pressing section as the demonstrations include force magnitudes along z, allowing the controller to partially shift the emphasis from impedance control to force control. A similar reduction of stiffness happens in the button task for the section of the trajectory that the button is pressed (plots are skipped for brevity).

The generated 9D trajectories were then fed to three different controllers to evaluate the performance of each with and without disturbance in the task environment. The disturbance consisted of lowering the button for 30mm in the button task and lowering the surface on which the tool was pressed for 35mm as well as moving the button laterally for 5mm in the peg-in-hole task. These disturbances are pictured in Figure 2. The following three controllers were deployed:

- **Imp:** Basic impedance controller (Eq. (4)) with fixed stiffness and damping.
- **Imp + FF:** Variable impedance control with force feed forward (Eq. (5)) and passivity observer.
- **Proposed:** The proposed controller (Eq. (25))

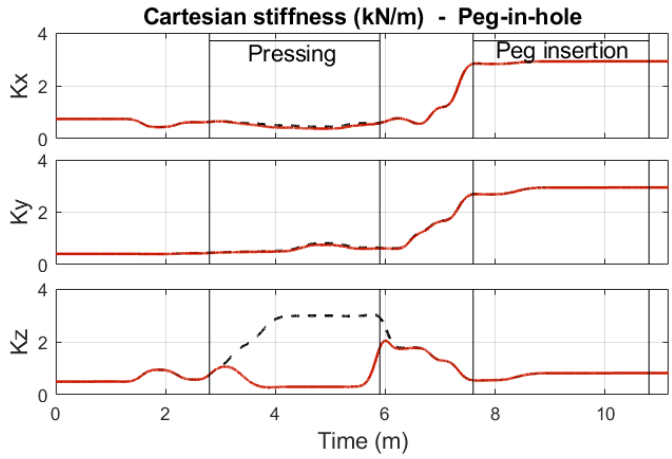

Figure 4 Generated Cartesian stiffnesses for the peg-in-hole task based on the variance of the demonstrated position trajectories shown as dashed line. Solid line represents the stiffness values reduced after considering the interaction forces recorded during the demonstration.

For the sake of brevity, we report only the measured forces along the z direction, out of the 6 dimensions of desired position and force. Nonetheless, for the considered tasks of this paper the interaction force along the z can concisely represent the performance of each controller without loss of generality of the derived conclusions. Left column of the plots in Figure 5 demonstrate the desired and measured forces during the reproduction of the button pressing task without disturbance. The sharp peaks seen in the Imp + FF and Proposed cases are due to successful engagement of the button, which includes a spring mechanism that is engaged when the button is pressed down with an adequate magnitude of force. The force exerted by the basic Imp controller relies merely on the position error and controller stiffness, which in this task is found to be insufficient to engage the button. This shortcoming is addressed by the addition of force feedforward in the Imp+FF controller. However, when the button is lowered it is only the proposed controller that succeeds in engaging the button, thanks to the additional force feedback term, as shown in the right column of the plots in Figure 5. In the case of the Imp controller the tool does not contact the button when lowered, as it relies only on position references.

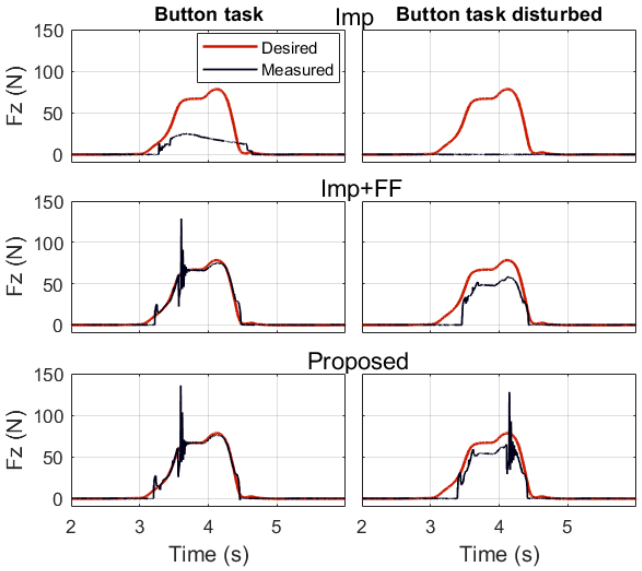

Figure 5 Recorded forces while different controllers reproduced the button task with and without disturbance. The sharp peaks refer to the button being successfully engaged.

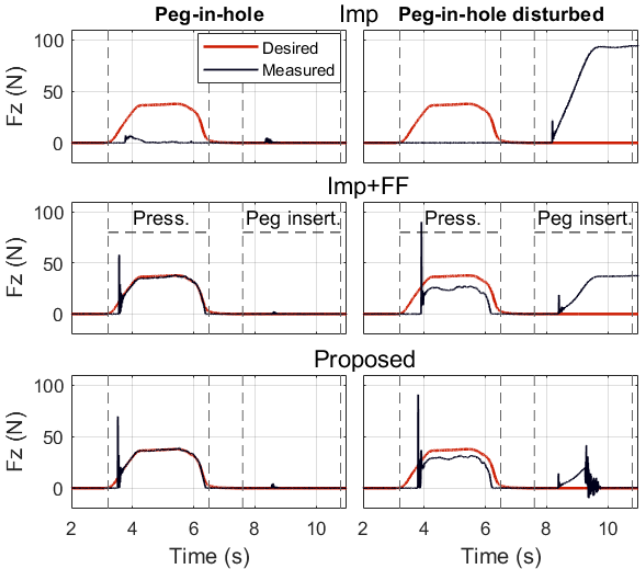

Figure 6 The recorded interaction forces along z during the reproduction of the peg-in-hole task by different controllers, with and without disturbance. The high magnitudes in the peg insertion phase seen in the impedance and impedance + force feedforward controllers plots for the disturbed setup is due to failure in insertion and pushing down on the side of the hole surface.

Figure 6 shows the encountered z forces in the peg-in-hole task. This task included a rigid surface pressing section to objectively evaluate force tracking performance and a peg-in-hole insertion to test robustness to geometrical uncertainties. As expected, the basic impedance controller did not produce the pressing forces on the surface, as the error in desired position tracking was mostly negligible. The other two controllers closely tracked the desired forces in the

undisturbed case. All three controllers succeeded in inserting the peg in the undisturbed case. However, when the hole was moved in the disturbed case, both the Imp and Imp + FF controllers collided with the flat side of the hole entrance (like shown in image D in Figure 2) and gradually increased the vertical force until saturation, thus failing in inserting the peg. The proposed controller succeeds in inserting the peg after an initial collision with the hole entrance surface. This is because the controller attempted to track the desired force reference that is zero in all 3 dimensions, however, the collision generated non-zero measured force. In this case, the effort of the controller to reduce the lateral measured forces (with respect to the axis of the cylindrical hole) lead to an eventual insertion of the peg. Note that in case of a flat peg tip, only vertical forces might be faced which can prevent also the proposed controller from reproducing the insertion successfully. If no mechanical guidance in the task can be exploited towards successful execution, one might resort to search motions such as the spiral search. In terms of force tracking performance in the pressing section when the surface was lowered, the proposed controller resulted in a superior mean absolute tracking error of 6.8 N compared to that of 10.1 N for the Imp + FF controller. Table 1 summarizes the outcome of the reproduction of each task by the controllers.

Table 1. Success in reproduction of experimental tasks using different controllers

	Imp.	**Imp. + FF**	**Proposed**
Button press	Fail	Success	Success
Peg-in-hole	Part-fail	Success	Success
Button press **disturbed**	Fail	Fail	Success
Peg-in-hole **disturbed**	Fail	Fail	Success

4. CONCLUSIONS

In this work we proposed an approach to simplify programming tasks that include interaction with the environment and to enhance the robustness of replicating such a programmed task. The proposed approach uses a single controller for contact and non-contact cases, preventing issues of controller switching. Through passivity analysis and a simulation, we demonstrated the stability of the proposed controller and experimental results validated its position and force tracking performance as compared to the state-of-the-art solutions. Extensions to include orientation and interaction wrenches are potential directions for future work.

5. REFERENCES

Argall, Brenna D., Sonia Chernova, Manuela Veloso, and Brett Browning. 2009. "A Survey of Robot Learning from Demonstration." *Robotics and Autonomous Systems* 57(5):469–83.

Billard, Aude, Sylvain Calinon, Rüdiger Dillmann, and Stefan Schaal. 2008. "Robot Programming by Demonstration." Pp. 1371–94 in *Springer Handbook of Robotics*. Springer Berlin Heidelberg.

Bishop, Christopher M. 2006. *Pattern Recognition and Machine Learning*. Springer.

Buchli, Jonas, Freek Stulp, Evangelos Theodorou, and Stefan Schaal. 2011. "Learning Variable Impedance Control." *International Journal of Robotics Research* 30(7):820–33.

Calinon, Sylvain. 2016. "A Tutorial on Task-Parameterized Movement Learning and Retrieval." *Intelligent Service Robotics* 9(1):1–29.

Calinon, Sylvain, Florent D'Halluin, Eric L. Sauser, Darwin G. Caldwell, and Aude G. Billard. 2010. "Learning and Reproduction of Gestures by Imitation." *IEEE Robotics and Automation Magazine* 17(2):44–54.

Calinon, Sylvain, Florent Guenter, and Aude Billard. 2007. "On Learning, Representing, and Generalizing a Task in a Humanoid Robot." *IEEE Transactions on Systems, Man, and Cybernetics, Part B: Cybernetics* 37(2):286–98.

Ferraguti, Federica, Cristian Secchi, and Cesare Fantuzzi. 2013. "A Tank-Based Approach to Impedance Control with Variable Stiffness." *2013 IEEE International Conference on Robotics and Automation* 4948–53.

Hogan, Neville. 1985. "Impedance Control: An Approach to Manipulation." *Dynamic Systems, Measurement, and Control* 107(March 1985):1–24.

Khansari-Zadeh, S. Mohammad and Aude Billard. 2011. "Learning Stable Nonlinear Dynamical Systems with Gaussian Mixture Models." *IEEE Transactions on Robotics* 27(5):943–57.

Khatib, Oussama. 1995. "Inertial Properties in Robotic Manipulation: An Object-Level Framework." *The International Journal of Robotics Research* 14(1):19–36.

Kormushev, Petar, Sylvain Calinon, and Darwin G. Caldwell. 2011. "Imitation Learning of Positional and Force Skills Demonstrated via Kinesthetic Teaching and Haptic Input." *Advanced Robotics* 25(5):581–603.

Kronander, Klas and Aude Billard. 2012. "Online Learning of Varying Stiffness through Physical Human-Robot Interaction." Pp. 1842–49 in *Proceedings - IEEE International Conference on Robotics and Automation*. Institute of Electrical and Electronics Engineers Inc.

Kronander, Klas and Aude Billard. 2016. "Stability Considerations for Variable Impedance Control." *IEEE Transactions on Robotics* 32(5):1298–1305.

Moberg, Stig, Jonas Öhr, and Svante Gunnarsson. 2008. "A Benchmark Problem for Robust Control of a Multivariable Nonlinear Flexible Manipulator." *Proceedings of the 17th IFAC World Congress* 1206–11.

Montebelli, Alberto, Franz Steinmetz, and Ville Kyrki. 2015. "On Handing down Our Tools to Robots: Single-Phase Kinesthetic Teaching for Dynamic in-Contact Tasks." *Proceedings - IEEE International Conference on Robotics and Automation* 2015-June(June):5628–34.

Ott, Christian. 2008. *Cartesian Impedance Control of Redundant and Flexible-Joint Robots*. Springer Berlin Heidelberg.

Paraschos, Alexandros, Christian Daniel, Jan Peters, and Gerhard Neumann. 2013. "Probabilistic Movement Primitives." *Advances in Neural Information Processing Systems* 1–9.

Racca, Mattia, Joni Pajarinen, Alberto Montebelli, and Ville Kyrki. 2016. "Learning In-Contact Control Strategies from Demonstration." *IEEE International Conference on Intelligent Robots and Systems* 2016-Novem:688–95.

Schaal, Stefan. 2006. "Dynamic Movement Primitives -A Framework for Motor Control in Humans and Humanoid Robotics." *Adaptive Motion of Animals and Machines* 261–80.

Schindlbeck, Christopher and Sami Haddadin. 2015. "Unified Passivity-Based Cartesian Force/Impedance Control for Rigid and Flexible Joint Robots via Task-Energy Tanks." *Proceedings - IEEE International Conference on Robotics and Automation* 2015-June(June):440–47.

Shahriari, Erfan, Aljaz Kramberger, Andrej Gams, Ales Ude, and Sami Haddadin. 2017. "Adapting to Contacts: Energy Tanks and Task Energy for Passivity-Based Dynamic Movement Primitives." *IEEE-RAS International Conference on Humanoid Robots* 136–42.

Siciliano, Bruno, Lorenzo Sciavicco, Luigi Villani, and Giuseppe Oriolo. 2009. *Robotics: Modelling, Planning and Control*.

Zeng, Ganwen and Ahmad Hemami. 1997. "An Overview of Robot Force Control." *Robotica* 15:473–82.